DOI 10.4430/bgo00403

Satellite-based investigation of drought effect on vegetation health index: Beyşehir-Kaşakli Sub-Basin, Turkey

M.G. Gümüş[1] and S.S. Durduran[2]

[1] *Department of Geomatics Engineering, Faculty of Engineering, Niğde Ömer Halisdemir University, Niğde, Turkey*
[2] *Department of Geomatics Engineering, Faculty of Engineering, Necmettin Erbakan University, Konya, Turkey*

(Received: 14 April 2022; accepted: 22 August 2022; published online: 11 November 2022)

ABSTRACT In this study, drought status analyses of Beyşehir-Kaşaklı Sub-Basin were carried out in the 35-year period (1984-2018) using remote sensing techniques, and accordingly, climate change factors were investigated. In this context, Landsat TM, ETM+, and OLI/TIRS were used. *LST, NDVI, VCI, TCI*, and *VHI* indexes were used as satellite-based drought monitoring techniques. Drought analyses were examined separately both for the basin in general and for the immediate surroundings of the Beyşehir and Seydişehir districts, the two largest districts of the basin. According to the results of drought categories evaluated by the *VHI*, Beyşehir and its surroundings and the entire basin underwent the highest droughts in 1985, 2000, and 2006. For Seydişehir and its surroundings, 1985, 1996, and 2000 were found to be the highest drought years. In addition, we sought to determine by variance analyses whether there is a statistically significant difference between the result values of *VHI* for different years. When the results of parametric and non-parametric variance analyses are examined, both variances show a statistically significant difference between *VHI* values for different years according to the analysis method.

Key words: drought monitoring, Landsat, remote sensing, variance analyses, vegetation health index.

1. Introduction

Natural disasters are defined as disasters that affect societies and human life by occurring for natural and human reasons, causing material as well as immaterial damage (Durduran and Geymen, 2008; Özşahin, 2013). Natural disasters continue to exist, with negative effects ranging from death, injury, economic crises, environmental destruction to more psychological problems in societies.

Countries have been planning numerous preparations to protect themselves from natural disasters, especially in recent years (Kızılelma and Karabulut, 2016). Of the 31 different types of natural disasters, 28 are meteorological. The types and severity of these disasters vary from country to country (AFAD, 2019). Drought, which is among the natural disasters of a meteorological nature, is the type of calamity having the most important domain compared to other natural disasters, for sustaining vital activities (Ding *et al*., 2011; Hillier, 2012; Dubovyk *et al*., 2019; Kale, 2021b). In general, drought is defined as the lack of water experienced in a certain period or the below average amount of water during a certain time (Altin *et al*., 2020;

Kumanlioglu, 2020). Drought occurs due to factors causing water scarcity, such as precipitation below average, excessive use of limited water resources, and irresponsible irrigation activities, and, as a result, environmental, agricultural, and socio-economic drought effects occur (Gümüş and Algin, 2017). Drought takes time to be noticed as it progresses very slowly. Since the beginning and end are not wholly predictable, it is separated from other natural disasters. The negative effects it creates cumulatively increase and last for longer periods of time, leading to major environmental disasters that can last for years even after the drought ends (Dogan *et al*., 2012). For this reason, detecting and monitoring of drought is a difficult process.

Drought is divided into groups according to its duration and formation. Regarding the duration, droughts are defined as short-term when effective for less than 6 months and long-term for more than 6 months (Dogan, 2013). Droughts are classified into certain classes by their formation, taking into account the variables such as precipitation, temperature, humidity, groundwater level, and the factors arising with these variables. These are classified as meteorological, agricultural, hydrological, and socio-economic droughts (Wilhite and Glantz, 1985). Generally, a drought situation begins with a meteorological drought. Meteorological drought is defined as precipitation below the normal value by deviating from the climate normals over a long period of time (minimum 30 years). Meteorological drought is regional, that is, it differs for each region. Sometimes differences can be observed even within the same region. Meteorological drought triggers agricultural drought and, therefore, hydrological drought. Agricultural drought is expressed as 'the situation in which there is not enough moisture in the root zone of the plant to grow and develop' (MGM, 2021). During the growth process of a plant, the decrease in soil moisture by deviating from its normal value and the lack of sufficient soil moisture cause agricultural drought. During dry periods, the amount of water in the soil and then the water amount of the plant decreases; in the next stages, the turgor pressure in the plant decreases, stomata are closed, photosynthesis is not possible, and plant growth slows down (Monti, 1986). The decrease in precipitation, low humidity values, the difference between actual and potential evapotranspiration, sudden increases in temperatures and drying winds, are all factors that exacerbate this type of drought (MEVKA, 2012). Hydrological drought, defined as a decrease below the normal value in surface and ground waters as one of the natural consequences of meteorological drought, can be observed with the lack of precipitation lasting for long periods. It is frequently witnessed at the basin scale. Hydrological drought decreases the flow rates of rivers, streams and canals. The water levels in lakes, dams and groundwaters decrease. Continuous monitoring and measurement of surface water resources and groundwater levels is required for the determination of hydrological drought effects. However, hydrological measurements cannot be the determining factor in the early detection of drought, since there is a delay between the lack of precipitation and the lack of water at the surface and groundwater levels. It takes time for reductions in precipitation to be noticed in the hydrological system. Even if the meteorological drought ends, the hydrological drought can continue its effect for long periods. As a result of meteorological, agricultural and hydrological droughts, socio-economic droughts are triggered. Socio-economic drought refers to the negative socio-economic consequences caused by all these types of drought (Wilhite and Glantz, 1985; Karabulut, 2015).

There is no single drought index defined for all drought activities on Earth due to its study and examination by different disciplines. It varies by geographical region depending on several parameters such as duration, frequency, type, range, and severity, and as the physical geography and climatology of each region show different drought trends and tendencies. Numerous different models and indications have been developed to determine and monitor drought types in the drought analysis process. Among the most commonly used are the Standardised

Precipitation Index [*SPI*, (McKee *et al*. (1993)], the Palmer Drought Severity Index (Palmer, 1965), the Standardised Precipitation Evapotranspiration Index [*SPEI*, Vicente-Serrano *et al*. (2015)], the Vegetation Health Index [*VHI*, Kogan (1997)], and the Vegetation Condition Index [*VCI*, Kogan (1990)]. Drought indices are an important tool for using statistical calculations and determining drought levels. Inscriptions are used to determine drought; this presents an objective criterion for uncovering climate change and its effects on any geographical region, detecting periods of drought in past years, warnings about drought, and taking measures (Türkeş and Tatlı, 2011).

Traditionally, the drought monitoring technique was based on meteorological and hydrological measurements obtained from regional measuring stations. Although the measurement data obtained from the stations are highly accurate, they are not very suitable for long-term (continuous) drought monitoring studies due to sparse observation networks, scale discrepancies, inability to reach continuous measurement values in the data, observational deficiencies in the data of the previous years, and validity for small-scale regional areas (Wang *et al.*, 2015). For this reason, remote sensing using satellites and location-specific drought monitoring may prove an appropriate option to minimise these disadvantages (Kucukmehmetoglu and Geymen, 2008; Sheffield *et al*., 2012; Köylü and Geymen, 2016; Bento *et al*., 2018; Vyas *et al*., 2020). Satellite-based drought indices are often used to acquire information about the current state of vegetation, land, soil, and surface waters. Using the different wavelengths in the electromagnetic spectrum, various mathematical formulae are applied to the reflection available values according to the subject of study, and calculations are made by obtaining a single value for each pixel. For example, the higher the values obtained when analysing the plant condition, the higher the plant density, and the lower the plant condition.

Among the satellite-based drought analysis methods performed with remote sensing data, the *VHI* index is widely used in the literature (Singh *et al*., 2003; Bhuiyan *et al*., 2006; Karnieli *et al*., 2006; Prasad *et al*., 2006; Quiring and Ganesh, 2010; Vicente-Serrano *et al*., 2010; Kogan *et al*., 2012; Ezzine *et al*., 2014; Bokusheva *et al*., 2016; Gouveia *et al*., 2017; Alamdarloo *et al*., 2018; Brito *et al*., 2018; Gidey *et al*., 2018; Pei *et al*., 2018; Wu *et al*., 2019).

The *VHI* index uses the visible (*VIR*), near-infrared (*NIR*) and thermal bands of the electromagnetic spectrum and is a container index type consisting of a linear combination of *TCI* (Temperature Condition Index) and *VCI* components. In the study of Bento *et al*. (2018), they investigated the active roles of *NDVI* (Normalised Differential Vegetation Index) and *LST* (Land Surface Temperature) using the *VHI* on arid regions and also systematically compared the relationship between the *VHI* and the *SPEI*. Sholihah *et al*. (2016) detected agricultural droughts with the *VHI* index using Landsat satellite imagery. Zeng *et al*. (2022) conducted an optimisation study to improve the global drought monitoring capacity of the *VHI*. Li *et al*. (2020) used *VHI* to explain crop growing status and yield in their study. Ekundayo *et al*. (2021) used *VHI* and annual SPI to determine the size and severity of spatial-temporal drought in the working area and investigated the correlation between the two indexes.

The main purpose of this study is to carry out drought situation analyses of the Beyşehir-Kaşaklı Sub-Basin (BKSB), using remote sensing and Geographic Information System techniques in the 35-year period covering 1984-2018 and to investigate climate change factors.

In the latest report of the International Panel on Climate Change (IPCC, 2013), it was announced that the Mediterranean Basin is one of the most sensitive regions to be affected by climate change (IPCC, 2007; Bayer Altin and Altin, 2021). Turkey is one of the Mediterranean countries most affected by climate change in the effective and efficient use of land. Especially between 1900 and 2005, significant drought trends were detected in the Mediterranean Basin

(Türkeş and Erlat, 2003; Türkeş and Tatlı, 2011; Kale, 2021a). The study area, BKSB, is located in this sensitive region with Mediterranean climate characteristics. The region is exposed to permanent deformations, especially in the last 50 years, due to factors such as the drying up of many important water resources including the Çarşamba Stream in the basin, agricultural irrigation activities and irresponsible water use, sudden decrease in precipitation and gradual warming of the land surface. It is very important to make sustainable designs and plans in order to determine these deformations in the basin and to eliminate the problems that occur as a result of these deformations. Therefore, for sustainable land management, all existing aspects of the land should be investigated and examined in detail. Due to the abovementioned reasons, BKSB has the status of an important basin where climatic change factors should be examined. In addition, there is no comprehensive analysis in the literature related to the drought situation in this region. It also plays an important role in the selection of BKSB as a study area, due to the limited drought studies in the region.

The article focuses on three different topics. Firstly, by conducting a land surveying study, the realisation of the regression analysis of the thermal data obtained from the terrestrial measurements and the satellite thermal values; then, the drought situation analysis by using the satellite-based *VHI* of the drought situation between 1985 and 2018 with the remote sensing method; finally, the *VHI* includes the evaluation of whether there is a significant change between the result data of different years obtained with the index and the analysis of variance.

2. Materials and methods

2.1. Study area

Turkey's largest closed basin, the Konya Closed Basin (KCB), is a strategically important basin accounting for 7% of the country's total area and approximately 14% of its agricultural land potential. BKSB, one of the nine sub-basins in the SW of the KCB, covers a fairly large area of approximately 7300 km^2. BKSB is located between 37° 26' - 38° 03' N and 31° 15' - 31° 46' E (Fig. 1).

The most important water resources of the basin are Beyşehir Lake, Suğla storage Lake, and Çarşamba River. Beyşehir Lake is the third largest lake in terms of surface area after Van and Tuz lakes and the largest freshwater lake in Turkey. Beyşehir Lake and its surroundings were declared a National Park by the Ministry of Forestry in 1993 under two different names: Beyşehir and Kızıldağ National Park. The region is a wetland in group A of international importance according to the Ramsar convention. The lake and its surroundings are also extremely important in terms of cultural and historical heritage, which is protected as a natural site area in the first, second, and third degree.

There are 19 meteorological stations operating in the basin. Among these, there are two stations where we can access the very old data archive for most parameters. These are Beyşehir (17242) and Seydişehir (17898) meteorological observation stations. BKSB is the sub-basin with the highest precipitation and the highest precipitation average in the KCB. In the Beyşehir (upper part of the basin) and Seydişehir (lower part of the basin) regions in the basin, the annual total precipitation reaches 750 mm. It has been recorded that the Seydişehir meteorological station receives approximately twice the average annual precipitation compared to the KCB. If this station is ignored, the average rainfall decreases from 380 mm to 347 mm. The summer months are hotter and drier, and the amount of precipitation is observed at a minimum level.

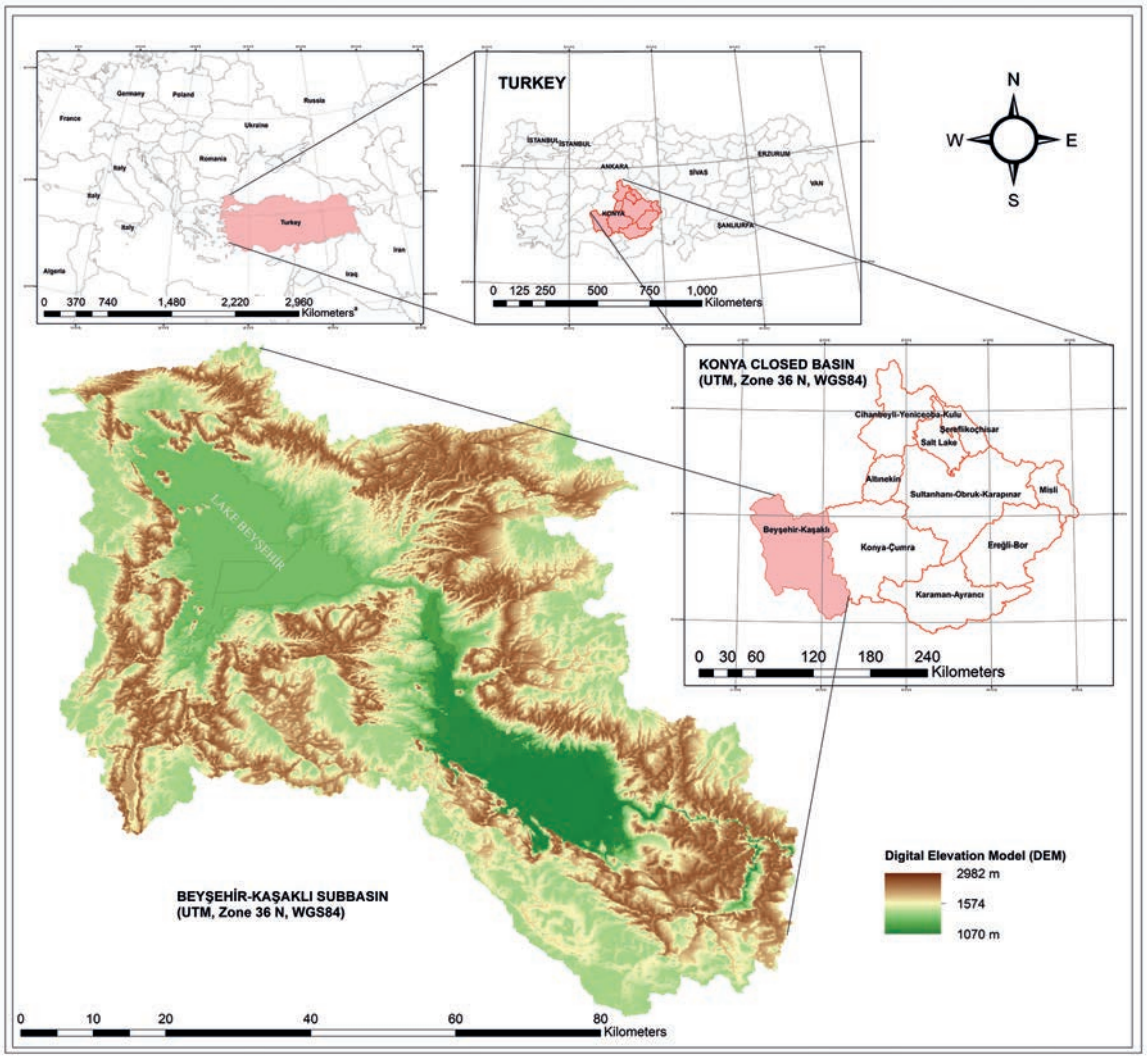

Fig. 1 - Representation the location and boundary of the BKSB.

The annual average temperature ranges from -0.4°C to 23.0°C. The highest temperature values of the year are observed in July and August. The coldest months are observed in January and February. The monthly and annual total precipitation data recorded in the observation period for the years 1970–2019, supplied by the General Directorate of Meteorology, are presented in Fig. 2. In addition, the average annual relative humidity of the basin was determined as 71% (Dalgıç, 2019). The prevailing wind direction of the basin blows in the S-SW direction (3.3 m/s). The fastest wind measurement was observed in March. It was recorded in the S-SW direction at a speed of 23.4 m/s. The average wind speed is 1.3 m/s (Anonymous, 1999; Yavuz, 2011).

The main reasons for choosing the BKSB as a working area are the increased agricultural irrigation activities and wasteful water use in recent years; sudden changes in precipitation and temperature increasing instances of drought; drying up of most of the 27 streams and streams feeding the lake; decreasing biodiversity in the lake; increased coastal erosion and accumulation. As a result, it is an important basin that needs attention due to both physical and human-

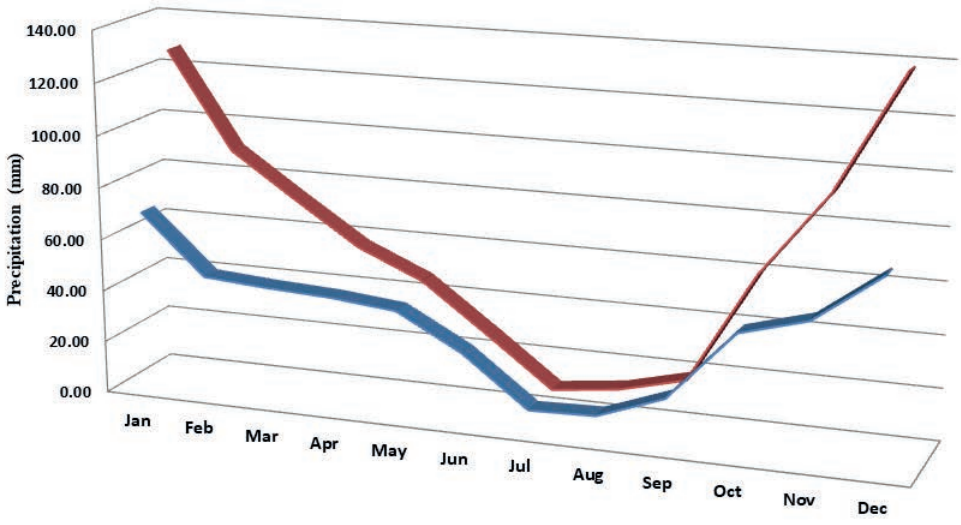

	Jan	Feb	Mar	Apr	May	Jun	Jul	Aug	Sep	Oct	Nov	Dec	Total (mm/year)
BEYS	69.92	47.15	45.33	44.07	41.58	28.14	9.14	9.93	19.32	46.38	53.43	72.12	486.51
SYDS	127.59	90.28	73.33	56.96	46.15	27.86	9.04	12.06	18.39	60.81	92.74	138.10	753.31

Fig. 2 - Monthly and annual total precipitation data of the basin (1970-2019).

induced changes such as irregular exchange activities along the coastal border. In addition, the fact that there was no comprehensive analysis of the drought situation of this region and that such studies in general in the region were very limited played an important role in the selection of basins.

2.2. The used data

Landsat TM (Thematic Mapper), ETM+ (Enhanced Thematic Mapper), and OLI (Operational Land Imager) / TIRS (Thermal Infrared Sensor) satellite images from 1984 to 2018 were used to analyse the drought status of the working area. Landsat-5 TM, Landsat-7 ETM+, Landsat-8 OLI/TIRS are visible and displayed in near-infrared (VNIR), short wave infrared (SWIR) and thermal infrared (TIR) ranges and have a medium spatial resolution between 15 and 100 m, depending on the spectral range. Their temporal resolution is 16 days. Spatial resolution spectral bands have a radiometric resolution of 30 m and a height of 705 km. Unlike Landsat-5, Landsat-7 carries a thematic mapper scanner. In addition to the standard 7 bands, the panchromatic band (0.50-0.90 µm) with a resolution of 15 m was added, and the resolution of the thermal band was reduced from 120 m to 60 m. Landsat-8 joined Landsat-7 in orbit in 2013, providing scientific data. Landsat-8's OLI sensor carries deep blue band for coastal/aerosol operations and a short-wave infrared band for cirrus clouds detection alongside previous bands. OLI collects data in nine spectral bands (Coastal/Aerosol + VNIR + SWIR + PAN + CIRRUS). Seven of these 9 bands have ranges found in previous Landsat-5 TM and Landsat-7 ETM+ sensors, ensuring that they are compatible with older Landsat data. The technical specifications (Schedule 2.1) of the Landsat satellite images used in the study are described in Table 1.

Table 1 - Used Landsat satellite images and technical specifications.

Sensors	Band Characteristics (μm)	Spatial Resolution (m)	Swath width (km^2)	WRS-2 (177/34) Date acquired	(178/34)
Landsat-5 TM*	1: 0.45-0.52	30	185 × 170	*10.08.1984	*16.07.1984
Landsat-7 ETM**	2: 0.52-0.60			*26.07.1990	*02.08.1990
	3: 0.63-0.69			*26.07.1996	*02.08.1996
	4: 0.76-0.90			*23.08.2006	*30.08.2006
	5: 1.55-1.75			*21.08.2011	*28.08.2011
	7: 2.082.35			**14.08.2000	**05.08.2000
	6: 10.1-12.50	120			
	6: 10.1-12.50	60			
	pan: 0.52-0.90	15			
Landsat-8 OLI/TIRS	1: 0.43-0.45	30	185 × 170	24.08.2018	15.08.2018
	2: 0.45-0.51				
	3: 0.53-0.59				
	4: 0.64-0.67				
	5: 1.85-1.88				
	7: 2.11- 2.29				
	9: 1.36-1.38				
	10: 10.60-11.19	100			
	11: 11.50-12.51	100			
	pan: 0.50-0.68	15			

Satellite images used in this study were provided free of charge by the USGS (2019). BKSB covers two full-frame Landsat images. The path/row numbers in the WRS-2 (The Worldwide Reference System) directory system for these two frame images are 177/34 and 178/34. Landsat satellite images have a medium spatial resolution, are frequently preferred in the detection of environmental changes, provide sufficient knowledge and information in a wide range of applications, and are provided free of charge.

2.3. Satellite-based drought index methods

2.3.1. Land Surface Temperature (*LST*)

It has been determined that surface energy and water balance are one of the most important parameters in the physical processes in both global and regional study areas (Brunsell and Gillies, 2003; Solanky *et al.*, 2018). *LST* plays an important role in climate change, drought situational determination and is widely used in hydrological, meteorological, agricultural and climatic applications.

LST is difficult to obtain with high accuracy from remotely-sensed raw TIR data since the irradiance measured by sensors depends not only on surface parameters (emission, temperature) but also on atmospheric effects, therefore, radiometric calibration and cloudiness, as well as atmospheric correction are required (Vidal, 1991). The first step used in the calculation of *LST* values is the radiometric correction process. The aim is to convert the digital number values obtained from satellite data into spectral radiance values. Eq. 1 used for this operation is as

follows:

$$L\lambda = \left[\frac{L_{MAX\lambda} - L_{MIN\lambda}}{QCAL_{MAX} - QCAL_{MIN}}\right] * [QCAL - QCAL_{MIN}] + L_{MIN} \quad (1)$$

where $L\lambda$ is the spectral radiance value at the sensor [W/(m²×sr×µm)], $L_{MAX\lambda}$ is the spectral radiance value scaled to $QCAL_{MAX}$, $L_{MIN\lambda}$ is the spectral radiance value scaled to $QCAL_{MIN}$, $QCAL$ is the brightness values, $QCAL_{MAX}$ is the maximum brightness value, and $QCAL_{MIN}$ is the minimum brightness value.

The following equation is used to convert the spectral radiance values obtained by applying this mathematical model to the actual *LST* values:

$$Tb = \frac{K_2}{\ln((\frac{K_1}{l\lambda})+1)} \quad (2)$$

where K_1 and K_2 are calibration constants and *Tb* is the surface temperature.

Finally, the resulting surface temperature is converted to degrees, and *LST* values are obtained:

$$LST = Tb - 273 \text{ (Kelvin to Degree conversion)} \quad (3)$$

2.3.2. Normalised Differential Vegetation Index (*NDVI*)

Developed by Tucker (1979), *NSVI* is an index species that informs us about vegetation density using reflection differences in the red (*R*) and near-infrared (*NIR*) regions from visible bands in the electromagnetic spectrum. The healthy vegetation pattern reflects a large portion of the light in the near-infrared region, while in the visible area it absorbs light; similarly, in the unhealthy vegetation pattern, it reflects the visible light more while reflecting less close infrared rays. This amount of reflection varies according to the pigments found in the plant leaves in the visible area and the cell structure in the near-infrared region (Molavizadeh *et al*., 2016). The mathematical formula used to calculate the *NDVI* value is (Rouse *et al*., 1974):

$$NDVI = (NIR - R)/(NIR + R). \quad (4)$$

The equation used in the study for the bands used for Landsat-5 and Landsat-7 is: *NDVI* = (Band 4 - Band 3) / (Band 4 + Band 3); for the bands used for Landsat-8 is: *NDVI* = (Band 5 - Band 4) / (Band 5 + Band 4). The values found as a result of *NDVI* analysis vary between -1 and +1. As the green plant density increases, the resulting value approaches +1, while as the plant density becomes sparse, this value approaches -1.

2.3.3. Vegetation Condition Index (*VCI*)

Although *NDVI* has successfully identified healthy and unhealthy plants, interpretation problems often arise due to changes in vegetation levels in a particular area and environmental sources such as climate, soil, and vegetation. The *NDVI* value alone makes it difficult to identify the climate component of crops, and researchers have designed the *VCI* index to easily determine the weather impact on crops (Kogan, 1990). The *VCI* is a function of minimum and maximum *NDVI*

values within long periods of vegetation density in a given ecosystem. *VCI* can be calculated by:

$$VCI = \frac{NDVI - NDVI_{min}}{NDVI_{max} - NDVI_{min}} \quad (5)$$

where the *VCI* value is between 0 and 1, or 0 and 100, these values determine the most frequently dense vegetation state.

2.3.4. Temperature Condition Index (*TCI*)

TCI is calculated using long-term temperature, very commonly used by various researchers to determine the stress of vegetation caused by temperature change (Nicholson, 1994). The calculation of *TCI* values is carried out conversely to *VCI* with:

$$TCI = \frac{T_{max} - T}{T_{max} - T_{min}} \quad (6)$$

considering that the increase in temperature will affect the development of vegetation. In such calculation, the values of both the *TCI* and *VCI* indices are of the same scale and size, and the increase in their values indicates a favorable situation for the crop.

Temperature conditions at any time are calculated using the maximum and minimum temperatures of the considered time. Low *TCI* values indicate adverse conditions for the crop, and high values indicate favorable conditions. When it comes to the crop, the temperature is most affected in the early stages of the crop, but a gradual increase in temperature indicates drought (Alahacoon *et al*., 2021).

2.3.5. Vegetation Health Index (*VHI*)

The *VHI* indicator, which combines *VCI* and *TCI* with the following Eq. 7, is designed to determine the health status of the crop. The *VCI* and *TCI* indices have an inverse relationship, i.e. the higher the *VCI* value, the lower the *TCI* value:

$$VHI = \alpha \times VCI + (1 - \alpha)TCI \quad (7)$$

where α is the contributing factor for both *VCI* and *TCI*. In most studies, the *VHI* drought index value is calculated by keeping it at 0.5, and the *VHI* value is distributed in the range of 0 to 100.

Table 2 - Classification of drought according to *VHI* values.

Values	Drought category
0-10	Extreme drought
10-20	Severe drought
20-30	Moderate drought
30-40	Mild drought
>40	No drought

Low *VHI* values indicate drought, while high values indicate dense vegetation. The results of the *VHI* equation are classified at the level of 5 droughts: no drought, mild, moderate, severe and extreme drought, as shown in Table 2 (Zuhro *et al*., 2020).

3. Results and discussion

NDVI, *LST*, *VCI*, *TCI*, and *VHI* indices were used in satellite-based drought analysis. Landsat (TM/ETM/OLI/TIRS) satellite images from 1985, 1990, 1996, 2000, 2006, 2012, and 2018 were used to perform satellite-based drought analyses. All analyses were performed using ENVI 5.3. (ENVI, 2015) and ArcGIS 10.5 (ESRI, 2018) software.

3.1. Land surveying

Before *LST* analyses were performed, simultaneous terrestrial measurements were performed in the study and regression analysis was carried out in order to determine the direction and strength of the linear relationship between them and satellite data. First, terrestrial measurements were made simultaneously between: 07:00 and 09:30 with the passage of Landsat-8 satellite image (path/row: 177/034) over the basin, which was obtained at start time 08:27:54 and end time 08:28:25. Terrestrial temperature data were obtained using an infrared thermometer from a total of 36 points containing different terrain types (woodland, herbaceous plants, field, moist soil, burned land, roads, etc.) during the specified time period. The point location information for the temperature values sampled was obtained using the CHCNAV I-80 GNSS receiver. All obtained data and attribute information are visualised in the ArcGIS environment (Fig. 3).

Forty-five repeated temperature measurements were performed from each point while making terrestrial measurements. The mean values obtained from these points were used in the analyses. Regression analysis was performed for the variables transferred to the numerical environment in order to reveal the relationship between the temperature data obtained by terrestrial measurements and the temperature data obtained from satellite data. For this purpose, the brightness values in Landsat-8 TIRS data have been converted to radiance values in order to compare the temperature data obtained with terrestrial measurements with satellite data. After the radiance values, *LST* values were obtained with the help of mathematical formulae. When the relationship between *LST* values obtained by converting from Landsat-8 TIRS data and mean temperature values obtained as a result of simultaneous terrestrial measurements from the field using an infrared thermometer was examined, it was determined that it had a positively high linear regression (Fig. 4).

It was determined that there was high coloration (R^2 0.8879) between the data obtained from Landsat-8 TIRS thermal satellite data used in August 2019 and the data obtained by simultaneously performed terrestrial measurements. This process demonstrated the reliability of the analyses made from *LST* data.

3.2. NDVI, LST, VCI, TCI and VHI analysis results

Visible, near-infrared, and thermal bands of Landsat-5 TM, Landsat-7 ETM, Landsat-8 TIRS satellite images were used to investigate changes in 1985, 1990, 1996, 2000, 2006, 2012, and 2018, to carry out satellite-based drought analyses. As a result of the analysis, *LST* of BKSB according to different years and the result maps obtained according to different increments were obtained (Fig. 5).

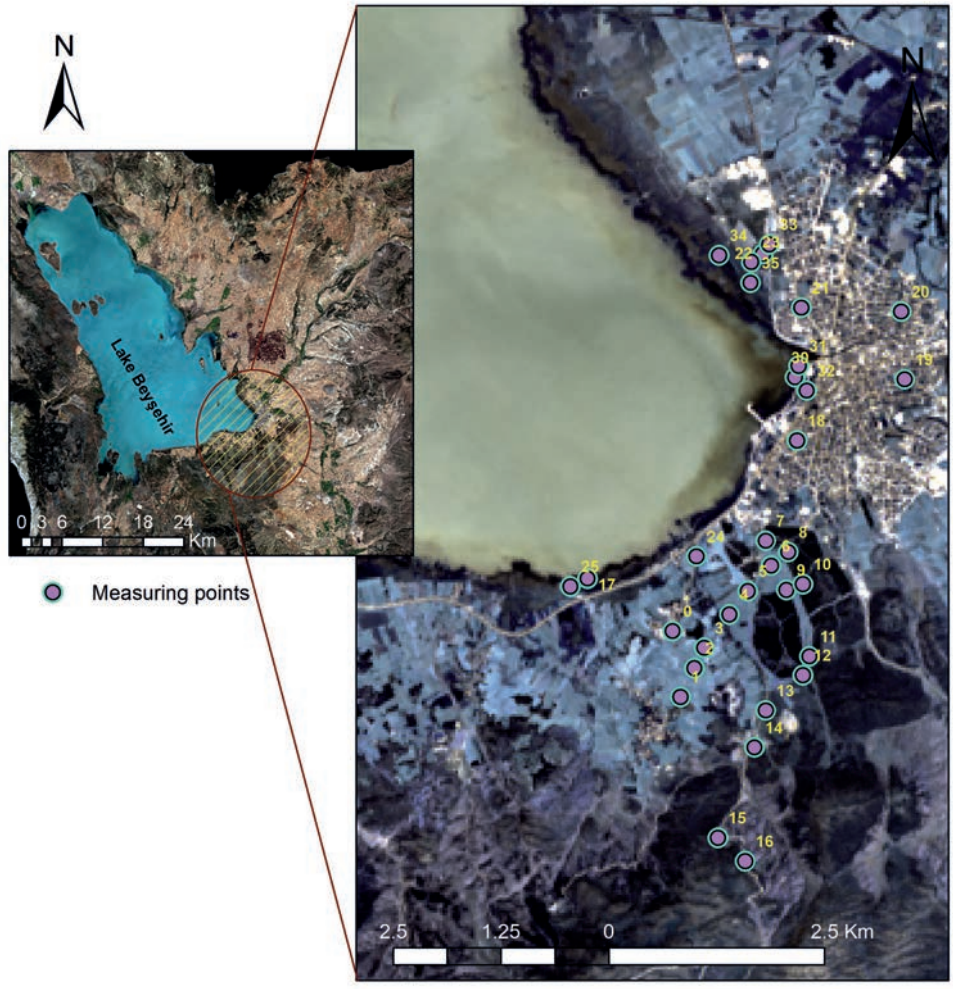

Fig. 3. - Measurement points taken for different terrain types.

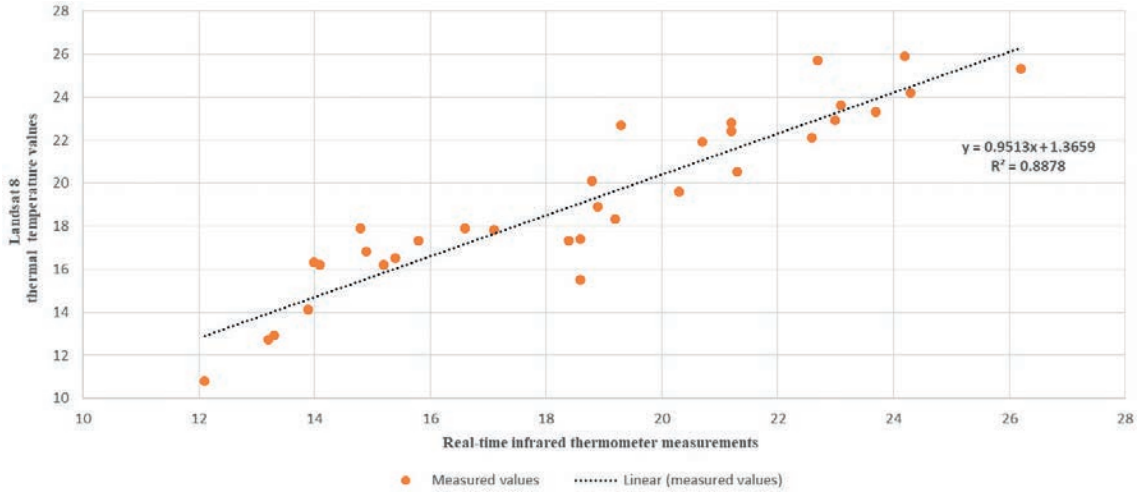

Fig. 4 - Regression analysis of simultaneous terrestrial and satellite data.

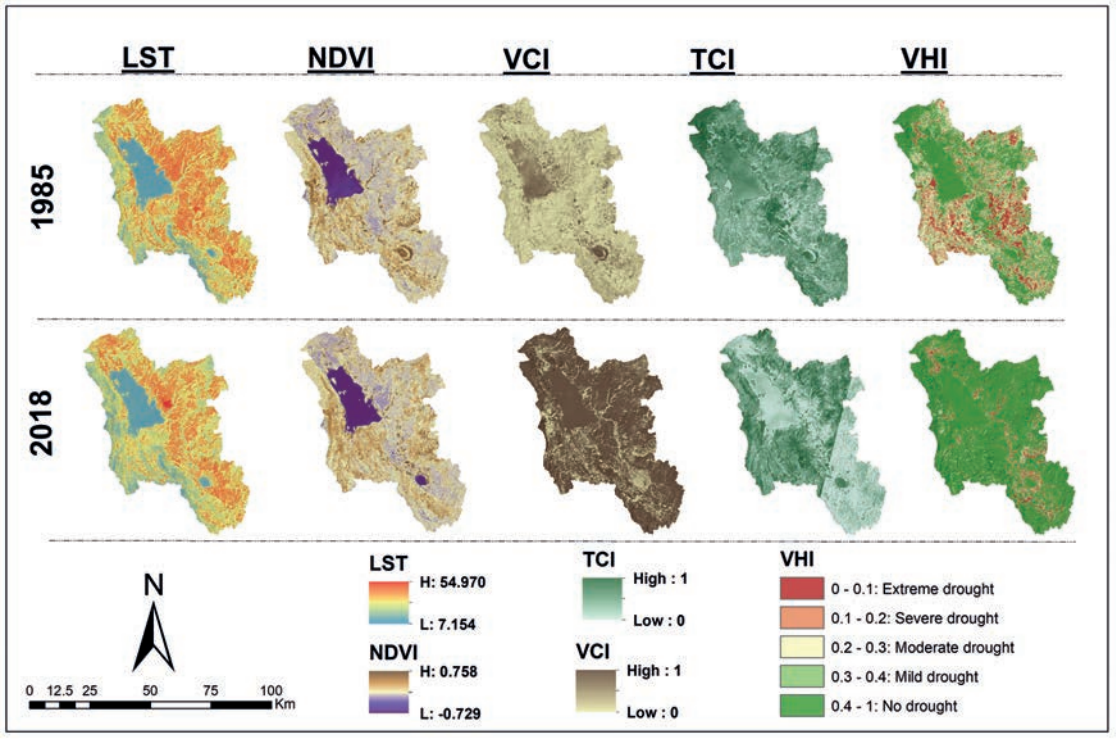

Fig. 5. - Drought analysis result maps obtained from different drought indexes.

Within the scope of the study, *VCI*, *TCI*, *NDVI*, *LST* and *VHI* maps were created as a result of satellite-based drought analyses and BKSB's drought status was revealed. In the interpretation of the maps, colouration analysis was applied to explain the current situation. In order to establish the colouration status between them, random points of 20×20 m^2 were defined throughout the basin in the ArcGIS. Drought values including drought index results are defined for the points created. All drought data obtained are automatically transferred to the attribute table for each point. Finally, the points created were cut off from the remaining ones within the basin boundary (Raster Clip) and the random points outside the basin boundary were removed. With this process, it is possible to examine the variations of the *VCI*, *TCI*, *NDVI*, *LST* and *VHI* values in each point by year by creating random points to cover the entire BKSB. *VCI*, *TCI*, *NDVI*, *LST* and *VHI* values corresponding to these points were obtained by estimating cutting maps from 1985, 1990, 1996, 2000, 2006, 2012 and 2018.

In addition, in order to examine the drought situation in more detail, random points were defined around the location of Beyşehir and Seydişehir stations as described above. The *VCI*, *TCI*, *NDVI*, *LST* and *VHI* values corresponding to these points were calculated on maps for 1985, 1990, 1996, 2000, 2006, 2012 and 2018. The values obtained according to different years and different methods are interpreted statistically both for the whole BKSB and for Beyşehir and Seydişehir environment. The full BKSB of the random points generated for the multipoint data assignment process is shown on the numerical terrain model for Beyşehir and Seydişehir immediate surroundings (Fig. 6).

The descriptive statistics of *VCI*, *TCI*, *NDVI*, *LST* and *VHI* values for 1985, 1990, 1996, 2000, 2006, 2012 and 2018 obtained for the entire BKSB, Beyşehir, and Seydişehir immediate vicinity are listed in Table 3.

Table 3 - The descriptive statistics of *VCI, TCI, NDVI, LST* and *VHI* values for different years.

Method	Year	Beyşehir			BKSB			Seydişehir		
		Min.	Max.	Mean	Min.	Max.	Mean	Min.	Max.	Mean
LST	1985	20.77	41.60	34.30	20.77	43.49	33.07	22.53	41.98	37.05
	1990	19.43	41.60	32.11	19.43	44.23	32.25	22.09	42.36	36.11
	1996	20.77	43.11	33.45	21.21	43.11	33.07	22.97	46.08	37.91
	2000	22.53	47.55	36.61	22.53	46.08	35.19	25.98	47.55	38.98
	2006	21.65	48.64	35.17	21.65	46.08	33.85	22.97	45.35	36.37
	2012	22.09	42.74	33.76	21.21	44.23	32.18	24.26	44.98	35.75
	2018	21.90	50.00	35.95	22.38	47.81	34.03	24.71	46.62	37.00
NDVI	1985	-0.36	0.55	0.05	-0.38	0.45	0.08	-0.23	0.60	0.09
	1990	-0.37	0.67	0.08	-0.41	0.50	0.10	-0.29	0.63	0.12
	1996	-0.32	0.69	0.10	-0.44	0.67	0.11	-0.38	0.67	0.13
	2000	-0.40	0.70	0.10	-0.46	0.66	0.12	-0.35	0.66	0.16
	2006	-0.51	0.65	0.05	-0.53	0.64	0.09	-0.33	0.66	0.12
	2012	-0.31	0.67	0.09	-0.47	0.64	0.13	-0.14	0.69	0.18
	2018	-0.19	0.54	0.14	-0.20	0.46	0.17	-0.18	0.60	0.19
TCI	1985	0.00	1.00	0.55	0.00	1.00	0.55	0.00	1.00	0.47
	1990	0.22	1.00	0.92	0.00	1.00	0.70	0.00	1.00	0.63
	1996	0.00	1.00	0.70	0.00	1.00	0.62	0.00	1.00	0.36
	2000	0.00	0.88	0.15	0.00	1.00	0.23	0.00	1.00	0.15
	2006	0.00	1.00	0.45	0.00	1.00	0.47	0.00	1.00	0.62
	2012	0.00	1.00	0.61	0.00	1.00	0.70	0.00	1.00	0.69
	2018	0.00	1.00	0.29	0.00	1.00	0.40	0.00	1.00	0.47
VCI	1985	0.00	1.00	0.22	0.00	1.00	0.17	0.00	1.00	0.14
	1990	0.00	1.00	0.41	0.00	1.00	0.33	0.00	1.00	0.31
	1996	0.00	1.00	0.47	0.00	1.00	0.45	0.00	1.00	0.36
	2000	0.00	1.00	0.48	0.00	1.00	0.39	0.00	1.00	0.51
	2006	0.00	1.00	0.18	0.00	1.00	0.25	0.00	1.00	0.26
	2012	0.00	1.00	0.45	0.00	1.00	0.61	0.00	1.00	0.62
	2018	0.00	1.00	0.86	0.00	1.00	0.80	0.00	1.00	0.77
VHI	1985	0.00	1.00	0.39	0.00	1.00	0.36	0.00	1.00	0.31
	1990	0.14	1.00	0.66	0.00	1.00	0.52	0.00	1.00	0.47
	1996	0.00	1.00	0.58	0.05	1.00	0.50	0.00	1.00	0.36
	2000	0.00	0.90	0.31	0.00	1.00	0.34	0.00	1.00	0.33
	2006	0.00	1.00	0.31	0.00	1.00	0.36	0.00	1.00	0.44
	2012	0.07	1.00	0.53	0.00	1.00	0.66	0.00	1.00	0.66
	2018	0.00	1.00	0.57	0.01	1.00	0.60	0.00	1.00	0.62

Using the average values of *VHI* and *LST* by year, combined graphs were created for the basin as a whole, Beyşehir, and Seydişehir. In these graphs, a comparison of different satellite-based drought indices with *LST* was made for different years. In general, these graphs are designed to determine how satellite-based *VHI* data are affected and varies over the years in the event of an increase or decrease in *LST*. When the combined graphs drawn from the average values of *VHI* and *LST* by year are examined, it is observed that satellite-based drought

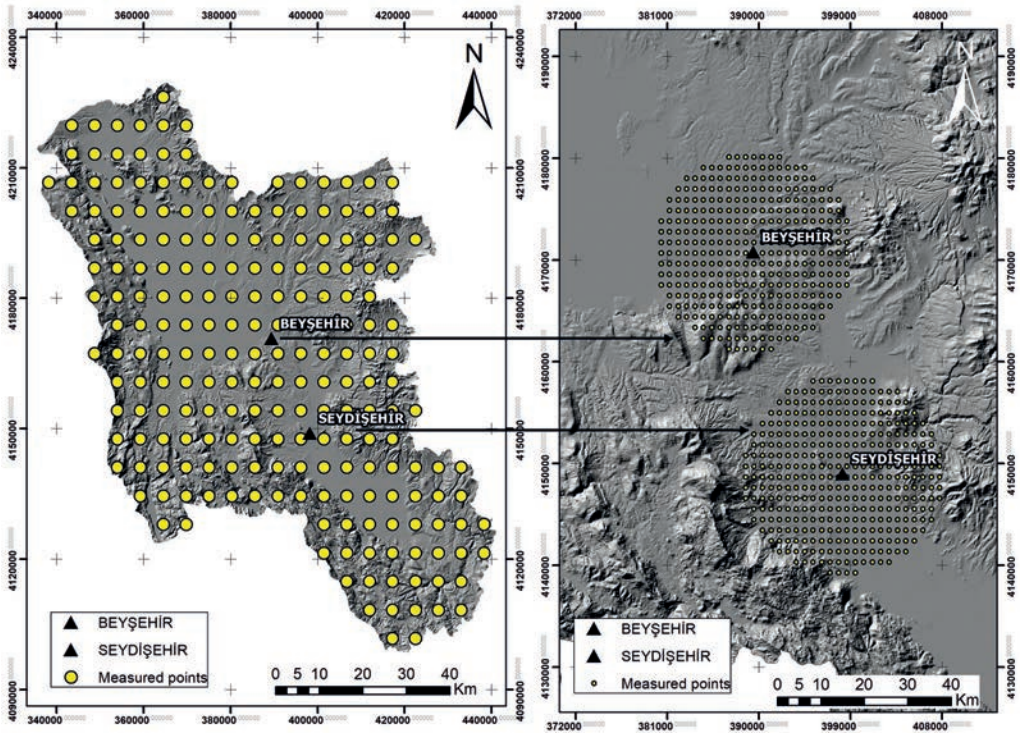

Fig. 6 - 20´20 m^2 random points placed in the whole of the basin, around Beyşehir and Seydişehir districts.

index values decrease as *LST* increases, and satellite-based drought index values increase as *LST* decreases (Fig. 7).

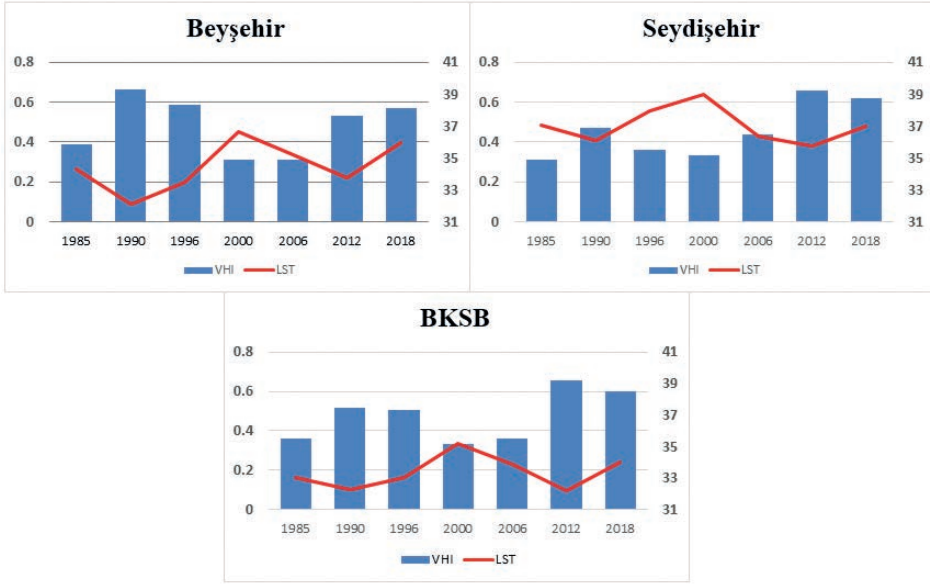

Fig. 7 - Comparison of *LST*-*VHI* values of different years.

In addition, the relationship between *TCI* and *VCI* was evaluated. A continuous decrease in *VCI* and *TCI* values or a constant low value is considered as an indicator of satellite-based droughts for a region or area. For this purpose, the comparison of the averages of *VCI* and *TCI* values for 1985, 1990, 1996, 2000, 2006, 2012 and 2018 obtained for the whole BKSB and for the surroundings of Beyşehir and Seydişehir, is shown in Fig. 8.

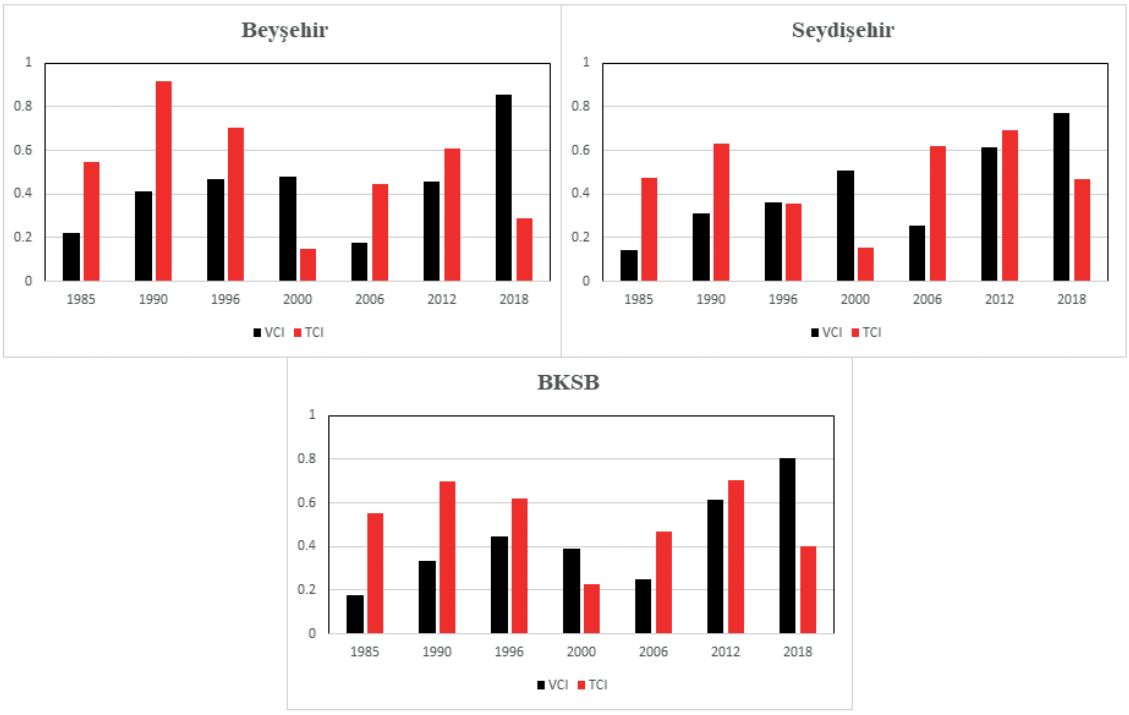

Fig. 8 - Comparison of *VCI* and *TCI* values.

When examining the *VCI* and *TCI* comparison charts of the different years, it was found that the *VCI* and *TCI* values give similar results in the basin and in the Beyşehir and Seydişehir regions. While the *TCI* value increases, the *VCI* value decreases and, in regions with decreased *TCI* value, it is observed that the *VCI* value increases with inverse proportion. In this case, it is understood that excessive temperature increase adversely affects the presence of vegetation.

In addition, we sought to determine whether there was a statistically significant difference between the values of *VHI* used to determine satellite-based droughts for 1985, 1990, 1996, 2000, 2006, 2012 and 2018. If there is a statistically significant difference, a one-way analysis of variance is performed to determine between which years this difference exists. The overall values of *VHI* for 1985, 1990, 1996, 2000, 2006, 2012 and 2018, were tested for normal distribution and homogeneity of groups before variance analysis was performed. In Table 4, the results of the homogeneity test of variances and the normal distribution test can be seen.

When the overall table is examined, it may be observed that the *VHI* values for different years are not normally distributed and the variances are not homogeneous because the *p*-value (Sig. in Table 4) is less than 0.05.

Table 4 - Variance homogeneity of *VHI* values and normal distribution test results.

The Normal Distribution Test						
	Kolmogorov-Smirnova			Shapiro-Wilk		
	Statistic	df	Sig.	Statistic	df	Sig.
Beyşehir	0.04	2450	0.00	0.99	2450	0.00
BKSB	0.03	1498	0.00	0.98	1498	0.00
Seydişehir	0.05	2478	0.00	0.97	2478	0.00
Variance Homogeneity Test						
	L. Statistic	df1		df2	Sig.	
Beyşehir	9.67	6		2443	0.00	
BKSB	10.28	6		1491	0.00	
Seydişehir	11.74	6		2471	0.00	

If the data are not normally distributed and homogeneous, non-parametric Kruskal Wallis variance analysis is required to determine whether there is a difference between *VHI* values and the averages of groups of different years. However, according to the literature, the results made by one-way variance analysis are healthier and the basic assumption of variance analysis is provided if the data are homogeneous and normally distributed. In this case, both Kruskal Wallis and one-way ANOVA (analysis of variance) testing were performed to determine whether there was a statistically significant difference between *VHI* values for different years (Tables 5 and 6).

Table 5 - Kruskal Wallis test results of *VHI* values.

Kruskal Wallis Test (Group variable: year)			
	Beyşehir	BKSB	Seydişehir
Chi-Square	782.38	329.30	533.09
df	6	6	6
Sig. (p)	0.00	0.00	0.00

Table 6 - One-way ANOVA test results of *VHI* values.

Unidirectional ANOVA - *VHI*						
Study area		Squares total	Freedom degree	Squares average	F	Sig.
Beyşehir	In-group	42.12	6	7.02	179.93	0.00
	Between groups	95.31	2443	0.04		
	Total	137.43	2449			
BKSB	In-group	20.99	6	3.50	70.93	0.00
	Between groups	73.52	1491	0.05		
	Total	94.50	1497			
Seydişehir	In-group	40.26	6	6.71	116.33	0.00
	Between groups	142.51	2471	0.06		
	Total	182.77	2477			

When Tables 5 and 6 are examined as a result of parametric and non-parametric variance analyses, it can be seen that the chart value of *F* at 95% significance level *p*-value (Sig. in the tables) is less than 0.05. This indicates a statistically significant difference between *VHI* values for different years according to both variance analysis methods. To determine in which years this difference between *VHI* values exists, pairwise comparisons were made by performing Post Hoc Test. For this purpose, Tamhane's T2 test was used because *VHI* data did not provide variance homogeneity. The list of those that do not have a statistically significant difference between the years is shown in Table 7, since the list of which the difference between them statistically makes sense in the resulting binary comparisons is very long.

Table 7 - *VHI* - Post Hoc Test - Pairwise Comparisons (Tamhane's T2).

VHI - Post Hoc Test- Pairwise Comparisons (Tamhane's T2)											
Beyşehir				**General**				**Seydişehir**			
(I)	**(J)**	**(I-J)**	**Sig.**	**(I)**	**(J)**	**(I-J)**	**Sig.**	**(I)**	**(J)**	**(I-J)**	**Sig.**
Year	**Year**	**Different**	**Sig.**	**Year**	**Year**	**Different**	**Sig.**	**Year**	**Year**	**Different**	**Sig.**
1996	2018	0.01	0.99	1985	2000	0.03	0.87	1985	2000	-0.02	0.92
2000	2006	0.00	1.00	1985	2006	0.00	1.00	1990	2006	0.03	0.56
2006	2000	0.00	1.00	1990	1996	0.01	1.00	1996	2000	0.03	0.69
2012	2018	-0.04	0.10	1996	1990	-0.01	1.00	2000	1985	0.02	0.92
2018	1996	-0.01	0.99	2000	1985	-0.03	0.87	2000	1996	-0.03	0.69
2018	2012	0.04	0.10	2000	2006	-0.02	0.93	2006	1990	-0.03	0.56
				2006	1985	0.00	1.00	2012	2018	0.04	0.43
				2006	2000	0.02	0.93	2018	2012	-0.04	0.43
				2012	2018	0.06	0.13				
				2018	2012	-0.06	0.13				

The mean differences were obtained from the averages related to the *VHI* dependent variable of the years. The significance levels are the *p*-values (Sig.) in Table 7. It was determined that there was no statistically significant difference between the years with significant levels above 0.05. There are statistically significant differences between the other years not listed in the table. These years have different *VHI* values, i.e. drought conditions due to these values. Table 8 shows averages and *p*-values (Sig.) for groups in subsets. With these subgroups, it is determined which years show the same or different characteristics according to *VHI* values. SPSS software has created subgroups for different years based on the *VHI* dependent variable. When the chart is examined, it should be noted that the *VHI* values or drought situations in the years included in the same group have similar characteristics, while the years in the other group show different characteristics.

In addition, *VHI* values obtained from satellite-based drought indexes according to different years are classified according to the drought categories described in the relevant section. This classification was carried out for 7 different years of 1985, 1990, 1996, 2000, 2006, 2012 and 2018, all of BKSB, Beyşehir and Seydişehir districts. The number and percentages of *VHI* drought classes for different years are given in Table 9.

Table 8 - Subgroups of different years for *VHI* values.

VHI - Subgroups															
Beyşehir						BKSB					Seydişehir				
Yıl	1	2	3	4	5	Yıl	1	2	3	4	Yıl	1	2	3	4
2006	0.31					2000	0.34				1985	0.31			
2000	0.31					2006	0.36				2000	0.33			
1985		0.39				1985	0.36				1996	0.36			
2012			0.53			1996		0.50			2006		0.44		
2018			0.57	0.57		1990		0.52			1990		0.47		
1996				0.58		2018			0.60		2018			0.62	
1990					0.66	2012			0.66		2012			0.66	
Sig.	1.00	1.00	0.10	0.99	1.00	Sig.	0.87	1.00	0.13		Sig.	0.09	0.56	0.43	

Table 9 - Number and percentages of drought classes obtained according to *VHI* values.

Drought classes		1985		1990		1996		2000		2006		2012		2018	
		N	%	N	%	N	%	N	%	N	%	N	%	N	%
BEYŞEHİR	Extreme dry	26	7.4	0	0	2	0.6	37	10.6	65	18.6	4	1.1	10	2.9
	Severe drought	29	8.3	2	0.6	5	1.4	74	21.1	65	18.6	19	5.4	8	2.3
	Moderate drought	51	14.6	3	0.9	20	5.7	70	20	55	15.7	31	8.9	13	3.7
	Mild drought	81	23.1	6	1.7	30	8.6	73	20.9	57	16.3	57	16.3	21	6
	No drought	163	46.6	339	96.9	293	83.7	96	27.4	108	30.9	239	68.3	298	85.1
	TOTAL	350	100	350	100	350	100	350	100	350	100	350	100	350	100
BKSB	Extreme dry	16	7.5	9	4.2	3	1.4	39	18.2	35	16.4	3	1.4	4	1.9
	Severe drought	28	13.1	12	5.6	3	1.4	36	16.8	26	12.1	13	6.1	8	3.7
	Moderate drought	41	19.2	16	7.5	20	9.3	32	15	33	15.4	15	7	9	4.2
	Mild drought	41	19.2	16	7.5	40	18.7	32	15	29	13.6	12	5.6	9	4.2
	No drought	88	41.1	161	75.2	148	69.2	75	35	91	42.5	171	79.9	184	86
	TOTAL	214	100	214	100	214	100	214	100	214	100	214	100	214	100
SEYDİŞEHİR	Extreme dry	75	21.1	22	6.2	37	10.4	39	11	54	15.2	6	1.7	13	3.7
	Severe drought	48	13.5	35	9.9	46	13	70	19.7	24	6.8	10	2.8	20	5.6
	Moderate drought	54	15.2	45	12.7	56	15.8	96	27	31	8.7	21	5.9	21	5.9
	Mild drought	51	14.4	29	8.2	85	23.9	58	16.3	36	10.1	35	9.9	21	5.9
	No drought	127	35.8	224	63.1	131	36.9	92	25.9	210	59.2	283	79.7	280	78.9
	TOTAL	355	100	355	100	355	100	355	100	355	100	355	100	355	100

According to Table 9, the annual drought status percentages, classified according to the *VHI* drought indexes, for the whole BKSB, the surroundings of Beyşehir, and Seydişehir are given in Table 10. Drought period for different years in the chart, the percentage ratio of the total number of extreme, severe, and moderate drought situations in the total data, and the Normal + humid period indicate the percentage equivalents of the drought status numbers of other drought categories in the total data.

Drought periods according to drought categories of different years are similar for Beyşehir and its surroundings and the whole of BKSB, while the percentages of drought periods are found

Table 10 - Drought situation percentages for the whole of BKSB, Beyşehir, and Seydişehir surroundings (%).

***VHI* - Drought situation percentages (%)**							
Beyşehir	**1985**	**1990**	**1996**	**2000**	**2006**	**2012**	**2018**
Dry period	53.4	3.1	16.3	72.6	69.1	31.7	14.9
Normal + humid period	46.6	96.9	83.7	27.4	30.9	68.3	85.1
Total	100	100	100	100	100	100	100
BKSB	**1985**	**1990**	**1996**	**2000**	**2006**	**2012**	**2018**
Dry period	58.9	24.8	30.8	65	57.5	20.1	14
Normal + humid period	41.1	75.2	69.2	35	42.5	79.9	86
Total	100	100	100	100	100	100	100
Seydişehir	**1985**	**1990**	**1996**	**2000**	**2006**	**2012**	**2018**
Dry period	64.2	36.9	63.1	74.1	40.8	20.3	21.1
Normal + humid period	35.8	63.1	36.9	25.9	59.2	79.7	78.9
Total	100	100	100	100	100	100	100

to differ from each other. The years 1985, 2000 and 2006 were designated as drought periods for Beyşehir and its surroundings and the whole of BKSB, and 1985, 1996, and 2000 for Seydişehir and its surroundings.

4. Conclusions

In this study, *NDVI*, *LST*, *VCI*, *TCI* and *VHI* indexes were used for satellite-based drought analysis. Landsat (TM/ETM/OLI/TIRS) satellite images from 1985, 1990, 1996, 2000, 2006, 2012 and 2018 were used to carry out satellite-based drought analyses. Before *LST* analyses were performed, simultaneous terrestrial measurements were performed to determine the direction and strength of the linear relationship between them and satellite data. It was determined that there was high colouration (R^2 0.8879) between the data obtained from Landsat-8 TIRS thermal satellite data used in August 2019 and the data obtained by simultaneously performed terrestrial measurements. This process demonstrated the reliability of the analyses made from *LST* data. Combined graphs drawn using the average values of *VHI* values and *LST* values by year were produced and a comparison of land surface temperature and different satellite-based drought indices was made according to different years. When the combined graphs are drawn from the average values of *VHI* satellite-based drought index values and *LST* values are examined, it can be observed that *VHI* values decrease as *LST* increases, and these values increase as *LST* decreases. In addition, we sought to determine whether there was a statistically significant difference between the values of *VHI* used to determine satellite-based droughts for 1985, 1990, 1996, 2000, 2006, 2012 and 2018, and variance analysis was applied for this purpose. Before variance analysis was performed, normal distribution and variances of groups were tested for homogeneity. When the test results were examined, it was found that the *VHI* values for different years were not normally distributed and the variances were not homogeneous because the *p* -value (Sig.) was less than 0.05. Both Kruskal Wallis and one-way ANOVA tests were performed to determine whether there was a statistically significant difference between *VHI* values. When the above charts are examined as a result of parametric and non-parametric variance analyses, it can be seen that the chart value of *F* at 95% significance level *p* value (Sig.) is less than 0.05. This

indicates a statistically significant difference between *VHI* values for different years according to both variance analysis methods.

In addition, *VHI* values obtained from satellite-based drought indexes according to different years are classified according to the drought categories described in the relevant section. This classification was carried out for 7 different years, namely 1985, 1990, 1996, 2000, 2006, 2012 and 2018, for all of BKSB, for Beyşehir and Seydişehir. Drought periods according to drought categories of different years are similar for Beyşehir and its surroundings and the whole of BKSB, while the percentages of drought periods are found to differ from each other. The years 1985, 2000, and 2006 were designated as dry periods for Beyşehir and its surroundings and the whole BKSB, while for Seydişehir and its surroundings dry periods correspond to years 1985, 1996, and 2000. According to satellite-based drought method results, it was determined that there were periods of severe drought especially between 1985-1990 and 2000-2006. 2006 was designated as the driest year in 35 years. The most humid years were found to have occurred between 1996 and 2012-2018.

The results obtained in this work have some similarities with previous academic studies. Sariş and Gedik (2021), using the SPI, found extreme droughts for similar years, especially in the Beyşehir and Seydişehir regions of the KCB. On the other hand, Türkeş *et al*. (2009), using the Palmer drought index, stated the start years of the dry period as 1970 and 2000. The analyses made in our study begin with the 1985 period. For this reason, it is consistent with the results of the dry periods (1985-1990 and 2000-2006). Orhan (2014), in his thesis study, which reveals the drought situation of the KCB by using meteorological and satellite-based drought analysis methods together, stated that the dry period started from 1982 and determined that the driest years were 1984 and 2008. In addition, according to the data obtained from meteorological observations between 1975 and 2011, it was determined that 55% of the region was arid. This is consistent with the results of our study. The similarity of the results presented in this paper with the previous academic studies indicates the soundness of the analyses.

In general, droughts hinder and destroy the sustainability of ecological systems ranging from agricultural activities to human life and public health, causing both material and psychological damage. Inclusive regional plans should be made to minimise or completely eradicate the effects of meteorological, agricultural and subsequent hydrological droughts. In the fight against drought, multidisciplinary research should be increased and regional development infrastructures should be prepared. In addition, reducing the planting of species with low tolerance to drought, replacing them with crops that are more resistant, will help prevent meteorological and, therefore, hydrological drought. In order to prevent hydrological droughts, regular measurements and continuous monitoring of hydrological drought parameters, including surface water resources and groundwater level measurements, are required from a managerial perspective.

Acknowledgments. This work was supported by the Necmettin Erbakan University Scientific Research Projects Unit (grant numbers 191419002). We also thank the United States Geological Survey (USGS) for supplying the Landsat satellite imagery used in the study.

REFERENCES

AFAD; 2019: *Disaster and Emergency Management Authority*, Ministry of Interior, Republic of Turkey, Ankara, Turkey, <www.afad.gov.tr/afadem/dogal-afetler>.

Alahacoon N., Edirisinghe M. and Ranagalage M.; 2021: *Satellite-based meteorological and agricultural drought monitoring for agricultural sustainability in Sri Lanka*. Sustainability, 13, 3427, doi: 10.3390/su13063427.

Alamdarloo E.H., Manesh M.B. and Khosravi H.; 2018: *Probability assessment of vegetation vulnerability to drought based on remote sensing data*. Environ. Monit. Assess., 190, 702, doi: 10.1007/s10661-018-7089-1.

Altin T.B., Sarış F. and Altın B.N.; 2020: *Determination of drought intensity in Seyhan and Ceyhan River basins, Turkey, by hydrological drought analysis*. Theor. Appl. Climatol., 139, 95-107, doi: 10.1007/s00704-019-02957-y.

Anonymous; 1999: *Beyşehir Lake wetland surface water collection basin management plan analytical study report*. Vols. 1, 2, 3, 4, 5, Tüstaş Sınai Tesisler A.Ş. Project Department, Ankara, Turkey, in Turkish.

Bayer Altin T. and Altin B.N.; 2021: *Response of hydrological drought to meteorological drought in the eastern Mediterranean Basin of Turkey*. J. Arid Land, 13, 470-486, doi: 10.1007/s4033 3-021-0064-7.

Bento V.A., Gouveia C.M., DaCamara C.C. and Trigo I.F.; 2018: *A climatological assessment of drought impact on vegetation health index*. Agric. For. Meteorol., 259, 286-295, doi: 10.1016/j.agrformet.2018.05.014.

Bhuiyan C., Singh R.P. and Kogan F.N.; 2006: *Monitoring drought dynamics in the Aravalli region (India) using different indices based on ground and remote sensing data*. Int. J. Appl. Earth Obs. Geoinf., 8, 289-302, doi: 10.1016/j.jag.2006.03.002.

Bokusheva R., Kogan F., Vitkovskaya I., Conradt S. and Batyrbayeva M.; 2016: *Satellite-based vegetation health indices as a criteria for insuring against drought-related yield losses*. Agric. For. Meteorol., 220, 200-206, doi: 10.1016/j.agrformet.2015.12.066.

Brito S.S.B., Cunha A.P.M.A., Cunningham C.C., Alvalá R.C., Marengo J.A. and Carvalho M.A.; 2018: *Frequency, duration and severity of drought in the Semiarid northeast Brazil region*. Int. J. Climatol., 38, 517-529, doi: 10.1002/joc.5225.

Brunsell N.A. and Gillies R.R.; 2003: *Length scale analysis of surface energy fluxes derived from remote sensing*. J. Hydrometeorol., 4, 1212-1219, doi: 10.1175/1525-7541(2003)004<12 12:LSAOSE>2.0.CO;2.

Dalgıç G.; 2019: *Coğrafi bilgi sistemleri ile Beyşehir Gölü havzasının ekolojik risk değerlendirmesi.* PH.D. Thesis in Applied Sciences, Graduate Education Institute, Isparta University of Applied Sciences, Isparta, Turkey, 109 pp.

Ding Y., Hayes M.J. and Widhalm M.; 2011: *Measuring economic impacts of drought: a review and discussion*. Disaster Prev. Manage., 20, 434-446, doi: 10.1108/09653561111161752.

Dogan S.; 2013: *Konya kapalı havzası kuraklık karakterizasyonunun zamansal-konumsal analizi.* PH.D. Thesis in Science and Technology, Institute of Science and Technology, Selcuk University, Konya, Turkey, 123 pp.

Dogan S., Berktay A. and Singh V.P.; 2012: *Comparison of multi-monthly rainfall-based drought severity indices, with application to semi-arid Konya closed basin. Turkey*. J. Hydrol., 470, 255-268, doi: 10.1016/j.jhydrol.2012.09.003.

Dubovyk O., Ghazaryan G., González J., Graw V., Löw F. and Schreier J.; 2019: *Drought hazard in Kazakhstan in 2000-2016: a remote sensing perspective*. Environ. Monit. Assess., 191, 510, doi: 10.1007/s10661-019-7620-z.

Durduran S.S. and Geymen A.; 2008: *Türkiyede Afet bilgi sistemi çalışmalarının genel bir değerlendirilmesi*. In: Proc. 2nd Remote Sensing and Geographic Information Systems Symposium, Erciyes University, Kayseri, Turkey, 9 pp.

Ekundayo O.Y., Okogbue E.C., Akinluyi F.O., Kalumba A.M. and Orimoloye I.R.; 2021: *Spatiotemporal drought assessment using vegetation health index and standardized precipitation index over Sudano-Sahelian region of Nigeria*. Afr. Geog. Rev., 40, 412-424, doi: 10.1080/19376812.2020.1841658.

ENVI; 2015: *ENVI Services Engine 5.3 User Guide*. <www.l3harrisgeo spatial.com/docs/pdf/ESE_help.pdf>, (Retrived January 2, 2021).

Environmental Systems Research Institute (ESRI); 2018: *ArcGIS Desktop 10.6 quick start guide*. <gisupdates.esri.com/ArcGIS/106pr/ArcGIS_106_Prerelease_Quick_ Start_Guides.pdf>, (Retrived January 27, 2021).

Ezzine H., Bouziane A. and Ouazar D.; 2014: *Seasonal comparisons of meteorological and agricultural drought indices in Morocco using open short time-series data*. Int. J. Appl. Earth Obs. Geoinf., 26, 36-48, doi: 10.1016/j.jag.2013.05.005.

Gidey E., Dikinya O., Sebego R., Segosebe E. and Zenebe A.; 2018: *Analysis of the long-term agricultural drought onset, cessation, duration, frequency, severity and spatial extent using Vegetation Health Index (VHI) in Raya and its environs, northern Ethiopia.* Environ. Syst. Res., 7, 1-18, doi: 10.1186/s40068-018-0115-z.

Gouveia C., Trigo R.M., Beguería S. and Vicente-Serrano S.M.; 2017: *Drought impacts on vegetation activity in the Mediterranean region: an assessment using remote sensing data and multi-scale drought indicators*. Global Planet. Change, 151, 15-27, doi: 10.1016/j.gloplacha.2016.06.011.

Gümüş V. and Algin H.M.; 2017: *Meteorological and hydrological drought analysis of the Seyhan-Ceyhan River basins, Turkey.* Meteorol. Appl., 24, 62-73, doi: 10.1002/met.1605.

Hillier D.; 2012: *A dangerous delay: the cost of late response to early warnings in the 2011 drought in the Horn of Africa*. Oxfami International, Oxford, UK, 58 pp.

IPCC (Intergovernmental Panel on Climate Change); 2007: *Climate change impacts, adaptation and vulnerability, fourth assessment report*. Contribution of Working Group II to the Fourth Assessment Report of the Intergovernmental Panel on Climate Change. Cambridge University Press, Cambridge, UK, 976 pp.

IPCC (Intergovernmental Panel on Climate Change); 2013: *Summary for policymakers*. In: Stocker T.F., Qin D., Plattner G.-K., Tignor M., Allen S.K., Boschung J., Nauels A., Xia Y., Bex V. and Midgley P.M. (eds), Climate change 2013: the physical science basis, Contribution of Working Group I to the Fifth Assessment Report of the Intergovernmental Panel on Climate Change, Cambridge University Press, Cambridge, UK, pp. 3-32.

Kale M.M.; 2021a: *Akarçay Kapalı Havzası için hidrolojik kuraklık analizi*. J. Geog., 42, 165-180, <dergipark.org.tr/en/pub/iucografya/issue/63677/892360>.

Kale M.M.; 2021b: *Manavgat çayı kuraklık analizi*. Aegean Geog. J., 30, 107-123, <dergipark.org.tr/en/pub/ecd/issue/63009/907303>.

Karabulut M.; 2015: *Drought analysis in Antakya-Kahramanmaraş Graben, Turkey*. J. Land, 7, 741-754, doi: 10.1007/s40333-015-0011-6.

Karnieli A., Bayasgalan M., Bayarjargal Y., Agam N., Khudulmur S., and Tucker C.J.; 2006: *Comments on the use of the vegetation health index over Mongolia*. Int. J. Remote Sens., 27, 2017-2024, doi: 10.1080/01431160500121727.

Kızılelma Y. and Karabulut M.; 2016: *Yozgat ve çevresinde kuraklık analizi*. In: Proc. International Bozok Symposium, Bozok University, Yozgat, Turkey, Vol. 4, pp. 242-251.

Kogan F.N.; 1990: *Remote sensing of weather impacts on vegetation in non-homogeneous areas*. Int. J. Remote Sens., 11, 1405-1419, doi: 10.1080/01431169008955102.

Kogan F.N.; 1997: *Global drought watch from space*. Bull. Am. Meteorol. Soc., 78, 621-636, doi: 10.1175/1520-0477(1997)078<0621:GDWFS>2.0.CO;2.

Kogan F., Salazar L. and Roytman L.; 2012: *Forecasting crop production using satellite-based vegetation health indices in Kansas, USA.* Int. J. Remote Sens., 33, 2798-2814, doi: 10.1080/01431161.2011.621464.

Köylü Ü. and Geymen A.; 2016: *GIS and remote sensing techniques for the assessment of the impact of land use change on runoff*. Arabian J. Geosci., 9, 1-12, doi: 10.1007/s12517-016-2514-7.

Kucukmehmetoglu M. and Geymen A.; 2008: *Measuring the spatial impacts of urbanization on the surface water resource basins in Istanbul via remote sensing*. Environ. Monit. Assess., 142, 153-169, doi: 10.1007/s10661-007-9917-6.

Kumanlioglu A.A.; 2020: *Characterizing meteorological and hydrological droughts: a case study of the Gediz River Basin, Turkey*. Meteorol. Appl., 27, e1857, doi: 10.1002/met.1857.

Li Y., Strapasson A. and Rojas O.; 2020: *Assessment of El Niño and La Niña impacts on China: enhancing the early warning system on food and agriculture*. Weather Clim. Extremes, 27, 100208, doi: 10.1016/j.wace.2019.100208.

McKee T.B., Doesken N.J. and Kleist J.; 1993: *The relationship of drought frequency and duration to time scales*. In: Proc. 8th Conference on Applied Climatology, Anaheim, CA, USA, pp. 179-183, <climate.colostate.edu/pdfs/relationshipofdroughtfrequency.pdf>.

Meteoroloji Genel Müdürlüğü (MGM); 2021: *Drought classes and their effects.* General Directorate of Meteorology, Ankara, Turkey, <www1.mgm.gov.tr/veridegerlendirme/kuraklik-analizi.aspx?d=yontemsinif> (Retrived 20 April 2021), in Turkish.

Mevlana Development Agency (MEVKA); 2012: *TR52 Region drought index.* Regional Research Reports Series, Publ. 4, p. 10, <www.mevka.org.tr/ Page.asp?Dil=0andpid=214> (Retrived April 2, 2021), in Turkish.

Molavizadeh N., Sertel E. and Demirel H.; 2016: *Drought conditions in Turkey between 2004 and 2013 via drought indices derived from remotely sensed data.* In: Green Energy and Technology, Springer, Cham, Switzerland, pp. 113-121. doi: 10.1007/978-3-319-30127-3_10.

Monti L.M.; 1986: *Breeding plants for drought resistance: the problem and its relevance, drought resistance in plants*. In: International Meeting on Advances on Phase Transitions and Disorder Phenomena, Amalfi, Italy, pp. 1-8.

Nicholson S.E.; 1994: *Recent rainfall fluctuations in Africa and their relationship to past conditions over the continent*. The Holocene, 4, 121-131, doi: 10.1177/095968369400400202.

Orhan O.; 2014: *Konya kapalı havzası'nda uzaktan algılama ve CBS teknolojileri ile iklim değişikliği ve kuraklık analizi.* PH.D. Thesis in Science and Technology, Institute of Science and Technology, Selcuk University, Aksaray, Turkey, 63 pp.

Özşahin E.; 2013: *Türkiye'de yaşanmiş (1970-2012) doğal afetler üzerine bir değerlendirme*. In: Proc. 2nd Turkey Earthquake Engineering and Seismology Conference, Hatay, Turkey, 8 pp., <www.tdmd.org.tr/TR/Genel/pdf/TDMSK046.pdf>.

Palmer W.C.; 1965: *Meteorological drought*. U.S. Department of Commerce, Weather Bureau, Washington, D.C., USA, Research paper 45, Vol. 30, 58 pp.

Pei F., Wu C., Liu X., Li X., Yang K., Zhou Y., Wang K., Xu L. and Xia G.; 2018: *Monitoring the vegetation activity in China using vegetation health indices.* Agric. For. Meteorol., 248, 215-227, doi: 10.1016/j.agrformet.2017.10.001.

Prasad A.K., Chai L., Singh R.P. and Kafatos M.; 2006: *Crop yield estimation model for Iowa using remote sensing and surface parame ters*. Int. J. Appl. Earth Obs. Geoinf., 8, 26-33, doi: 10.1016/j.jag.2005.06.002.

Quiring S.M. and Ganesh S.; 2010: *Evaluating the utility of the Vegetation Condition Index (VCI) for monitoring meteorological drought in Texas*. Agric. For. Meteorol., 150, 330-339, doi: 10.1016/j.agrformet.2009.11.015.

Rouse J.W., Haas R.H., Schell J.A. and Deering D.W.; 1974: *Monitoring vegetation systems in the Great Plains with ERTS*. In: Third ERTS-1 Symposium NASA, NASA SP-351, Washington, D.C., USA, pp. 309-317.

Sarış F. and Gedik F.; 2021: *Konya kapalı havzası'nda meteorolojik kuraklık analizi*. J. Geog., 42, 295-308, <dergipark.org.tr/en/pub/iucografya/issue/63677/885519#article_cite>.

Sheffield J., Wood E.F. and Roderick M.L.; 2012: *Little change in global drought over the past 60 years*. Nature, 491, 435-438, doi: 10.1038/nature11575.

Sholihah R.I., Trisasongko B.H., Shiddiq D., La Ode S.I., Kusdaryanto S. and Panuju D.R.; 2016: *Identification of agricultural drought extent based on vegetation health indices of landsat data: case of Subang and Karawang, Indonesia*. Procedia Environ. Sci., 33, 14-20, doi: 10.1016/j. proenv.2016.03.051.

Singh R.P., Roy S. and Kogan F.; 2003: *Vegetation and temperature condition indices from NOAA AVHRR data for drought monitoring over India.* Int. J. Remote Sens., 24, 4393-4402, doi: 10.1080/014311 6031000084323.

Solanky V., Singh S. and Katiyar S.K.; 2018: *Land surface temperature estimation using remote sensing data*. In: Hydrologic Modeling, Springer, Singapore, pp. 343-351, doi: 10.1007/978-981-10-5801-1_24.

Tucker C.J.; 1979: *Red and photographic infrared linear combinations for monitoring vegetation*. Remote Sens. Environ., 8, 127-150, doi: 10.1016/0034-4257(79)90013-0.

Türkeş M. and Erlat E.; 2003: *Precipitation changes and variability in Turkey linked to the North Atlantic oscillation during the period 1930-2000*. Int. J. Climatol., 23, 1771-1796, doi: 10.1002/joc.962.

Türkeş M. and Tatlı H.; 2011: *Use of the spectral clustering to determine coherent precipitation regions in Turkey for the period 1929-2007*. Int. J. Climatol., 31, 2055-2067, doi: 10.1002/joc.2212.

Türkeş M., Akgündüz S. and Demirörs Z.; 2009: *Palmer kuraklık İndisi'ne göre İç anadolu bölgesi'nin konya bölümü'ndeki kurak dönemler ve kuraklık şiddeti*. Turkish J. Geog. Sci., 7, 129-144, doi: 10.1501/Cogbil_0000000102.

USGS; 2019: *United States Geological Research Institute.* Reston, VA, USA, <earthexplorer.usgs.gov/>, (Retrieved 12 May 2021).

Vicente-Serrano S.M., Beguería S. and López-Moreno J.I.; 2010: *A multiscalar drought index sensitive to global warming: the standardized precipitation evapotranspiration index*. J. Clim., 23, 1696-1718, doi: 10.1175/2009JCLI2909.1.

Vicente-Serrano S.M., Van der Schrier G., Beguería S., Azorin-Molina C. and Lopez-Moreno J.I.; 2015: *Contribution of precipitation and reference evapotranspiration to drought indices under different climates*. J. Hydrol., 526, 42-54, doi: 10.1016/j.jhydrol.2014.11.025.

Vidal A.; 1991: *Atmospheric and emissivity correction of land surface temperature measured from satellite using ground measurements or satellite data*. Int. J. Remote Sens., 12, 2449-2460, doi: 10.1080/01431169108955279.

Vyas S.S. and Bhattacharya B.K.; 2020: *Agricultural drought early warning from geostationary meteorological satellites: concept and demonstration over semi-arid tract in India*. Environ. Monit. Assess., 192, 1-15, doi: 10.1007/s10661-020-08272-8.

Wang Q., Shi P., Lei T., Geng G., Liu J., Mo X., Li X., Zhou H. and Wu J.; 2015: *The alleviating trend of drought in the Huang-Huai-Hai Plain of China based on the daily SPEI*. Int. J. Climatol., 35, 3760-3769, doi: 10.1002/joc.4244.

Wilhite D.A. and Glantz M.H.; 1985: *Understanding the drought phenomenon: the role of definitions.* Water Int., 10, 111-120, doi: 10.1080/02508068508686328.

Wu Z., Yu L., Zhang X., Du Z. and Zhang H.; 2019: *Satellite-based large-scale vegetation dynamics in ecological restoration programmes of northern China*. Int. J. Remote Sens., 40, 2296-2312, doi: 10.1080/01431161.2018.1519286.

Yavuz F.; 2011: *Katılımcı havza planlaması ve yönetimi: Beyşehir Gölü havzası'nda kritik başarı faktörlerinin değerlendirilmesi*. PH.D. Thesis in Science and Technology, Institute of Science and Technology, Selcuk University, Konya,Turkey, 115 pp.

Zeng J., Zhang R., Qu Y., Zhou T., Lin Y., Wu X., Qi J., Shui W. and Wang Q.; 2022: *Improving the drought monitoring capability of VHI at the global scale via ensemble indices for various vegetation types from 2001 to 2018*. Weather Clim. Extremes, 35, 100412, doi: 10.1016/j.wace.2022.100412.

Zuhro A., Tambunan M.P. and Marko K.; 2020: *Application of vegetation health index (VHI) to identify distribution of agricultural drought in Indramayu Regency, west Java Province*. IOP Conference Series: Earth and Environmental Science, Vol. 500, 012047, <iopscience.iop.org/article/10.1088/1755-1315/500/1/012047/meta>.

Corresponding author: Münevver Gizem Gümüş
Department of Geomatics Engineering, Faculty of Engineering, Niğde Ömer Halisdemir University
Alparslan Türkeş street, Central Campus, Niğde,Turkey
Phone: +90 388 2254643; e-mail: gizemkisaaga@ohu.edu.tr